Sensitivity of the Factor of Safety of Railway Embankments to Saturated and Unsaturated Soil Properties

Gitirana Jr., G. F. N.
Universidade Federal de Goiás, Goiânia, GO, Brazil, gilsongj@eec.ufg.br

Fredlund, D. G.
Golder Associates Ltd., Saskatoon, SK, Canada, unsaturatedsoil@yahoo.com

Abstract: Weather-related mass movements have a significant impact on urban and rural areas. The assessment and management of geo-hazards involves the understanding of complex coupled unsaturated soil phenomena and numerous soil and weather parameters. Therefore, it becomes important to determine what parameters and mechanisms have significant impact to the stability of such slopes. The primary goal of this paper is to present the sensitivity of a series of hypothetical railway embankments to the controlling soil properties, particularly the unsaturated properties. A discrete probabilistic procedure is presented, using a moment-matching method. Probabilistic and deterministic event tornado diagrams are presented, showing the relative sensitivity to each parameter. It is shown that certain parameters have transient sensitivities and that the uncertainty of several soil properties can be neglected.

Resumo: Movimentos de massa relacionados com interferências atmosféricas produzem importantes impactos em zonas rurais e urbanas. A avaliação e gerenciamento destas ameaças geotécnicas requerem o entendimento de complexos fenômenos acoplados e numerosos parâmetros do solo e atmosféricos. Desta forma, se torna importante determinar quais parâmetros e mecanismos possuem impactos significantes na estabilidade de taludes. O objetivo principal deste artigo é apresentar a sensibilidade de uma série de aterros de linhas férreas hipotéticos, aos parâmetros do solo, particularmente os parâmetros do solo não saturado. Para tal, um procedimento probabilístico discreto é apresentado, utilizando um método de equivalência de momentos. Diagramas tornado determinísticos e probabilísticos são apresentados, demonstrando a sensibilidade relativa a cada parâmetro. É mostrado que certos parâmetros apresentam sensibilidades transientes e que a incerteza de várias propriedades pode ser ignorada.

Keywords: soil-atmosphere flux; slope stability; hazard assessment; soil-water characteristic curve.
Palavras-chave: fluxo solo-atmosfera; estabilidade de taludes; avaliação de risco; curva característica.

1 INTRODUCTION

Weather-related geo-hazards are a major concern for the railway industry in Canada. The financial losses that result from derailments and delays amount to millions of dollars every year. The safety exposure of employees and the public is also a concern. Many miles of Canadian railway subgrade are susceptible to embankment failure. The failure mechanisms often involve near-ground surface, unsaturated soils. Therefore, complex hydro-mechanical behavior and soil-atmosphere interactions must be understood.

According to the Transportation Safety Board (1997), the occurrence of railway subgrades composed of "moisture-sensitive" alluvial deposits reflects the limited construction capabilities and understanding of soil characteristics at the time of construction. Steps are required in order to identify, monitor, and modify "moisture-sensitive" embankments. Beaver control, culvert inspections, and adoption of modern construction standards are acknowledged remedial measures already in place.

Gitirana Jr. (2005) proposed a decision support system that can make use of information obtained from the monitoring of weather and unsaturated embankment conditions. The decision support system is capable of quantifying railway embankments hazards and can assist in indicating appropriate inspection frequencies, thereby providing a way to rationale railway resources.

One important step toward the implementation of such system is to determine what soil properties are more relevant to the slope failure. This paper presents a series of sensitivity analysis studies carried out considering hypothetical embankments. The contribution of the inherent variability of the saturated and unsaturated properties to the variability of the factor of safety is determined by means of tornado diagrams.

2 HAZARD ASSESSMENT MODEL

The development of a proactive hazards management system is a challenging task. Figure 1 presents the components of a management model for railway embankment hazards. According to Fig. 1, a decision making system must be established and entail: (i) risk quantification criteria, (ii) acceptable risk levels, and (iii) a collection of managing actions available. Risks are a function of hazard levels and potential hazard consequences. Therefore, a hazard management model requires a decision support system that is capable of providing a measure of embankment hazard.

2.1 Deterministic model

The thermo-hydro-mechanical behavior of the soil comprising a railway embankment can be represented by a system of partial differential equations (PDE's). These equations are obtained using a traditional continuum mechanics approach and appropriate state variables. The broadly accepted stress state variables; namely, net stress (σ–u_a) and matric suction (u_a–u_w), are used, where σ is the total stress, u_a is the pore-air pressure, and u_w is the pore-water pressure. The displacement state variables are the horizontal and vertical displacements, u and v (x- and y-direction, respectively), and the change in volume of water and air in a referential volume. The PDE's governing (i) static force equilibrium, (ii) flow of moisture, and (iii) flow of heat are obtained from basic continuity and equilibrium laws, combined with constitutive laws that describe soil behavior. Fredlund and Gitirana Jr. (2005) present an overview of these PDEs.

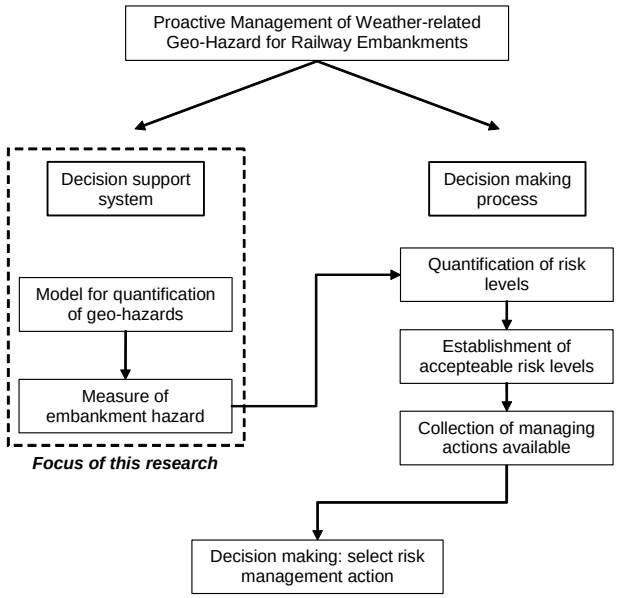

Figure 1. Components of a management model for railway embankment hazards

The computation of changes in water content and pore-water pressure distribution within an embankment form an essential step towards to the assessment of weather-related geo-hazards. Atmospheric forcing conditions produce internal moisture flow and changes in the pore-water pressures within the embankment. The internal flow makes moisture available for evaporation and/or allows precipitation to infiltrate the embankment. Neglecting either evaporation or infiltration may lead to unrealistic pore-water pressure predictions. The importance of taking into account evaporative fluxes is particularly evident in arid and semi-arid regions (Fredlund and Rahardjo, 1993).

The partial differential equations governing the flow and conservation of liquid water, water vapour, and heat must be solved taking into account soil-atmosphere forcing conditions. The stability of the railway embankment may be quantified at any time by computing the factor of safety.

A large number of soil properties are required in order to quantify geo-hazards; namely, k^w = hydraulic conductivity; k^v = vapour conductivity; n = porosity; ψ_b = air-entry value; λ_d = SWCC primary slope; λ_{res} = SWCC residual slope; λ_s = thermal conductivity of the soil; L_V = latent heat of vaporization; ζ = volumetric specific heat of soil; D_{ij} = stress-strain constitutive matrix terms; γ_{nat} = soil unit weight; c' = effective cohesion; ϕ' = effective friction angle; and κ = unsaturated shear strength parameter.

A computer code using the dynamic programming method (DPM) has been developed (Gitirana Jr. and Fredlund, 2003) for the analysis of embankment stability. The application of DPM to slope stability analyses has been first proposed by Baker (1980). Recent research has verified that the DPM provides factors of safety similar to those using the enhanced method and conventional methods of slices. However, more flexible, no-circular slip surfaces can be obtained. The occurrence of non-circular slip surfaces are a particular concern for the assessment of embankment hazards where sharp wetting fronts occur (Gitirana Jr. and Fredlund, 2003).

2.2 Probabilistic model

A formal probabilistic and sensitivity analysis framework has been established for the assessment of weather-related geo-hazards. The framework recognizes the paramount importance of taking into account unsaturated soil parameter uncertainty and provides an alternative approach, compatible with approximate unsaturated soil property functions.

A brief description of the probabilistic and sensitivity analysis framework will be presented herein, but a detailed description can be found in Gitirana Jr. (2005). The probabilistic framework is based on an alternative point estimate method,

APEM. The APEM is based on the combination of the Rosenblueth (1975) method and the Taylor series approximation. The approach is similar to that proposed by Li (1992). The equations proposed for uncorrelated variables are as follows:

$$E[F_s(X)] = F_s(E[X]) + \sum_{i=1}^{n}\left[p_i^+ F_s(x_i^+) + p_i^- F_s(x_i^-) - F_s(E[X])\right] \quad (1)$$

$$\mu_m[F_s(X)] = \left\{F_s(E[X]) - E[F_s(X)]\right\}^m + \sum_{i=1}^{n}\begin{bmatrix} p_i^+\left\{F_s(x_i^+) - E[F_s(X)]\right\}^m \\ + p_i^-\left\{F_s(x_i^-) - E[F_s(X)]\right\}^m \\ - \left\{F_s(E[X]) - E[F_s(X)]\right\}^m \end{bmatrix} \quad (2)$$

where F_s is the factor of safety, E[] is the first central moment, μ_m is the statistical moment of order m; $p_i = 0.5$ for the normal distribution; $F_s(x_i^{\pm}) = F_s(E[x_1],\ldots\ x_i^{\pm},\ldots\ E[x_n])$; $x_i^{\pm} = x_i \pm 1 \times \mathrm{SD}[x_i]$; $\mathrm{SD}[x_i]$ is the standard deviation of x_i; and n is the number of input random variables (uncertain soil properties).

Gitirana Jr. (2005) presents more general equations, considering skewed and correlated input variables. The first two statistical moments of F_s computed using Eqs. 1 and 2 can be used in the computation of the probability of failure, P_f. Equations 1 and 2 require a relatively small number of computations of F_s ($2n$+1 for uncorrelated variables), when compared to the Rosenblueth (1975) method (i.e., 2^n). For instance, the 12 input variables presented in the next section require 25 evaluations of F_s using the APEM, while 4096 evaluations would be required using Rosenblueth.

Equations 1 and 2 can also be used for sensitivity analyses. The sample points used by Equations 1 and 2 (i.e., $F_s(x_i^{\pm})$) provide measures of F_s that can be used in the construction of tornado diagrams. Tornado diagrams are commonly used in Decision Analysis and provide a formal approach for sensitivity analysis (Clemen, 1996). A deterministic tornado diagram shows the variability of F_s due to the uncertainty of each input random variable. The wider the resulting bar, the larger the uncertainty "transferred" to F_s by the input variable. Probabilistic tornado diagrams show the variability of F_s when the variability of one input variable is removed at a time. Therefore, the narrower bars indicate those properties whose uncertainties have the more significant impacts to the uncertainty of F_s.

3 CASE SCENARIOS

A series of hypothetical embankments were analyzed. The geometry and properties were selected in order to cover a wide range of typically found embankments along the CP Rail network. The hypothetical railway embankments were analyzed considering simple atmospheric conditions corresponding to a strong rainfall. Therefore, the vapour and heat flow components of the model are expected to play a negligible role. Gitirana Jr (2005) presents additional examples, for varying conditions, including periods of evapotranspiration.

The analysis model was implemented using a partial differential equation solver (FlexPDE, 2005), the dynamic programming code Safe-DP (Gitirana Jr., 2005), and spreadsheet routines for the APEM and sensitivity analysis computations.

Table 1. Soil parameters adopted for the simulations.

Analysis	Property (2)	Parameters (3)	Expected value (*)		CV (**)	
			Loam	Clay	Loam	Clay
Moisture flow analysis	$\theta = nS$	n	0.500	0.534	17%	17%
		$\ln(\psi_b)$, ln(kPa)	0.927 (2.50)	0.999 (2.71)	115%	115%
		$\ln(\lambda_d)$, $\ln(\ln(\mathrm{kPa})^{-1})$	-0.737 (0.50)	--	90%	--
		$\ln(\lambda_{res})$, $\ln(\ln(\mathrm{kPa})^{-1})$	-2.445 (0.090)	--	12%	--
	k^w	$\ln(k^w_{sat})$, ln(m/s)	-12.58 (3.5×10^{-6})	-16.03 (1.1×10^{-7})	15%	13%
	k^v	$\ln(D^v_{25}o_C)$, $\ln(m^2/s)$	-9.4 (8.33×10^{-5})	-9.4 (8.33×10^{-5})	15%	15%
Heat flow	λ	λ_s, W/(m °C)	6.0	6.0	25%	25%
Stress and stability analysis	D_{ij}	E, kPa	15,000	7,000	30%	30%
		μ	0.35	0.40	22%	17%
	τ_f	c', kPa	0.0	10.0	30%	30%
		ϕ'	30°	20°	10%	10%
		$\ln(\kappa)$	0 (1)	0 (1)	SD = 0.5	SD = 0.5

where: θ is the volumetric water content and S is the degree of saturation.
Fixed parameters: $a = 0.050$ (SWCC equation by Gitirana Jr. and Fredlund, 2004); $D_R = 2.65$;
$L_V = 2.501\times10^6 - 2.361\times10^3 T$ J/kg; $\zeta_s = 2.23\times10^6$ W/(m³ °C); $\zeta_w = 4.15\times10^6$ W/(m³ °C);
(*) values between brackets are the exponential values;
(**) values for which the mean is close to zero may have the variability indicated in terms of standard deviation, SD.

3.1 Geometry and soil properties

Figure 2 presents the geometry, initial, and boundary conditions adopted. Two embankments were analyzed, 5 and 15 meters high. Embankment side slopes at 1.5H:1.0V were selected, based on typical embankments found along the Canadian railway network. A relatively heavy train load of 28 kN/m^2 was adopted. The initial pore-water pressure conditions are based on a 1 m deep water table and a minimum pore-water pressure of -20 kPa, -60 kPa, and -100 kPa. A constant rainfall of 40 mm/day was applied during 14 days. This amount of precipitation is comparable to the precipitation and melted water anteceding a considerable number of railway embankment failures reported by the Transportation Safety Board (1997).

Table 1 presents the soil properties required and the values adopted herein. These values correspond to a lacustrine silt or loam, according to the USDA classification system. The hydraulic conductivity function, shear strength envelope, vapour conductivity function, thermal conductivity function, and heat capacity function were estimated based on the soil-water characteristic curve. Gitirana Jr. (2005) presents a detailed description of the estimation approaches available and the estimation techniques adopted for this study.

The shear strength envelope was predicted using the equation proposed by Fredlund et al. (1996):

$$\tau_f = c' + (\sigma_n - u_a)\tan\phi' + (u_a - u_w)S^{\kappa}\tan\phi' \qquad (3)$$

where c' is the soil cohesion, ϕ' is the friction angle, and κ is a fitting parameter.

Typical coefficients of variation were collected from the literature for the Young modulus, E, Poisson ratio, μ, effective cohesion, c', and friction angle, ϕ'.

The remaining parameters were statistically assessed using a large database of soils (SoilVision, 2003) and a statistical assessment methodology specially developed for unsaturated soil property functions (Gitirana Jr., 2005). A soil-water characteristic curve, SWCC, with independent parameter was selected (Gitirana Jr. and Fredlund, 2004). The parameters defining the SWCC are the air-entry value, ψ_b, the primary slope, λ_d, the residual slope, λ_{res}, and a parameter controlling the sharpness of the SWCC curvatures (a = 0.05). The parameters that are presented in terms of natural logarithm (see Table 1) are those determined to be log normally distributed.

The coefficient of variation of the diffusivity of water vapour, D^v_{25oC}, the thermal conductivity, λ_s, and the unsaturated shear strength parameter, κ, were assessed based on the three-sigma rule.

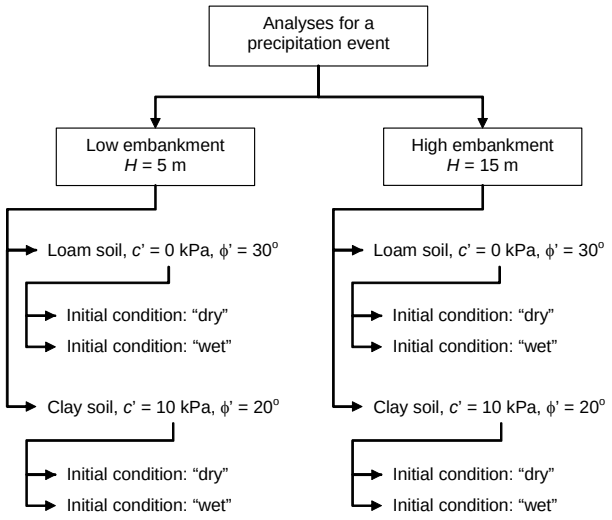

Figure 2. Embankment configurations.

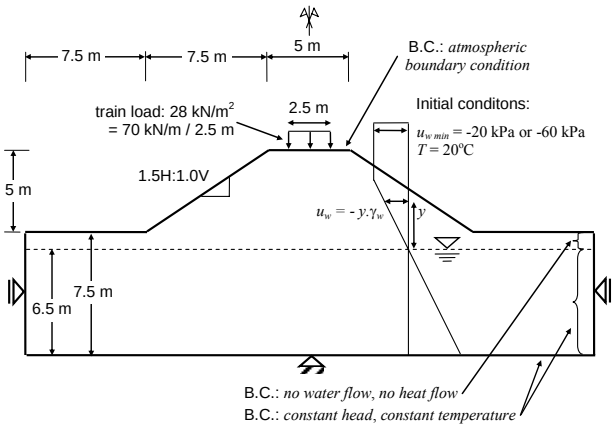

Figure 3. Low embankment.

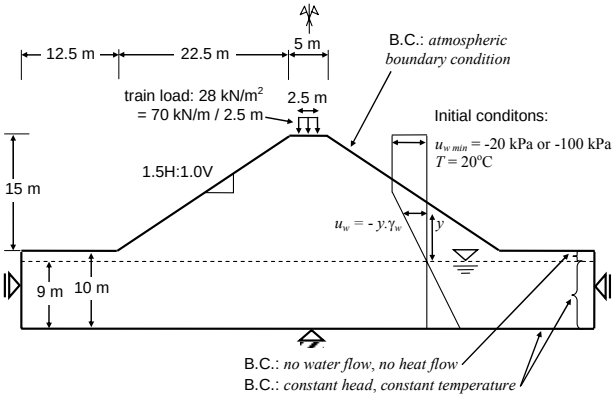

Figure 4. High embankment.

4 RESULTS AND DISCUSSION

This section presents the results of the sensitivity analysis for the case scenarios presented in the previous section. The term "sensitivity" is used throughout this section to refer to how much the uncertainty of the factor of safety is affected by the inherent uncertainty of a given input parameter.

4.1 Low loam embankments

Input variables such as the shear strength parameters and the elastic parameters have a direct influence in the factor of safety. However, soil parameters related to the flow of water and heat affect the factor of safety in an indirect manner, through changes in the pore-water pressure distribution with time.

Figure 5 presents the final pore-water pressure profiles (t = 14 days) for the mid-section of the low railway embankment considering two initial conditions (i.e., "dry" and "wet"). It can be observed that the wetting fronts are considerably deeper for the "wet" embankment, as expected.

Figure 5 presents also the profiles obtained using the estimate points (i.e., the ± 1 SD variations) for the saturated hydraulic conductivity and the air-entry value. An increase in the air-entry value resulted in higher pore-water pressures at greater depths and resulted in a smooth or non-existent wetting front. This effect was expected, since an increase in the air-entry value results in higher degrees of saturation and in a higher hydraulic conductivity for higher soil suctions. A smaller air-entry value resulted in a sharper wetting front and higher matric suctions at greater depths.

The effects of changes in the saturated hydraulic conductivity are also shown in Fig. 5. An increase in the saturated hydraulic conductivity resulted in the absence of a sharp wetting front. The negative pore-water pressure profile presents a constant value that increases as the soil saturates. The absence of a sharp wetting front resulted in higher soil suctions at the surface. Therefore, higher values of k^{w}_{sat} are expected to decrease the hazard levels.

Figure 6 presents deterministic event tornado diagrams at t = 14 days. The deterministic event tornado diagrams are obtained by adding the uncertainty of one variable at a time and computing the resulting variability of the factor of safety. The left and right coordinates of the bars presented in Fig. 6 correspond to the 10th and 90th percentiles of the factor of safety p.d.f.. The line on the middle of each bar corresponds to the 50th percentile. A lognormal distribution was assumed for the factor of safety. The larger the size of a bar, the more sensitive is the factor of safety to the input variable corresponding to that bar.

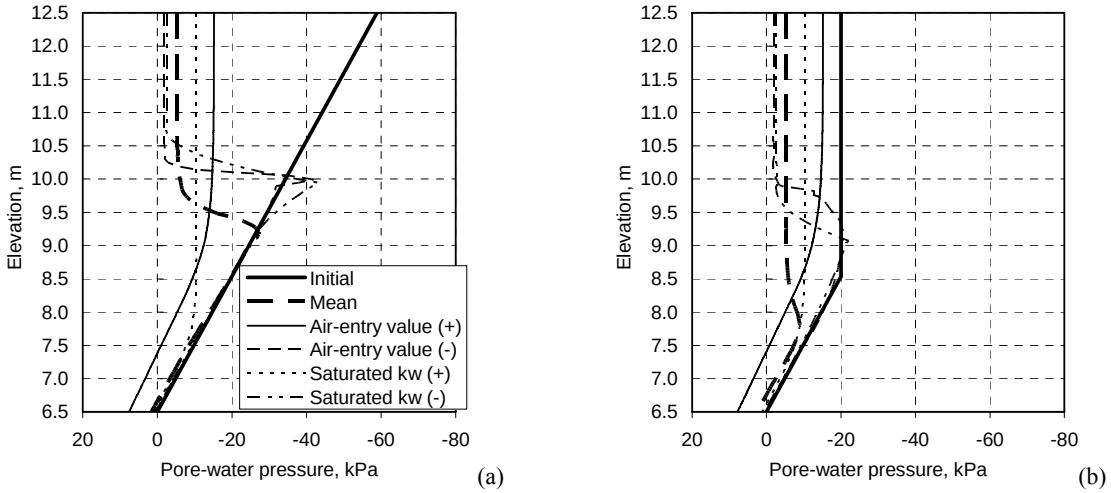

Figure 5. Pore-water pressure at the mid-section of the low, loam embankment: (a) u_{wmin} = -60 kPa; (b) u_{wmin} = -20 kPa.

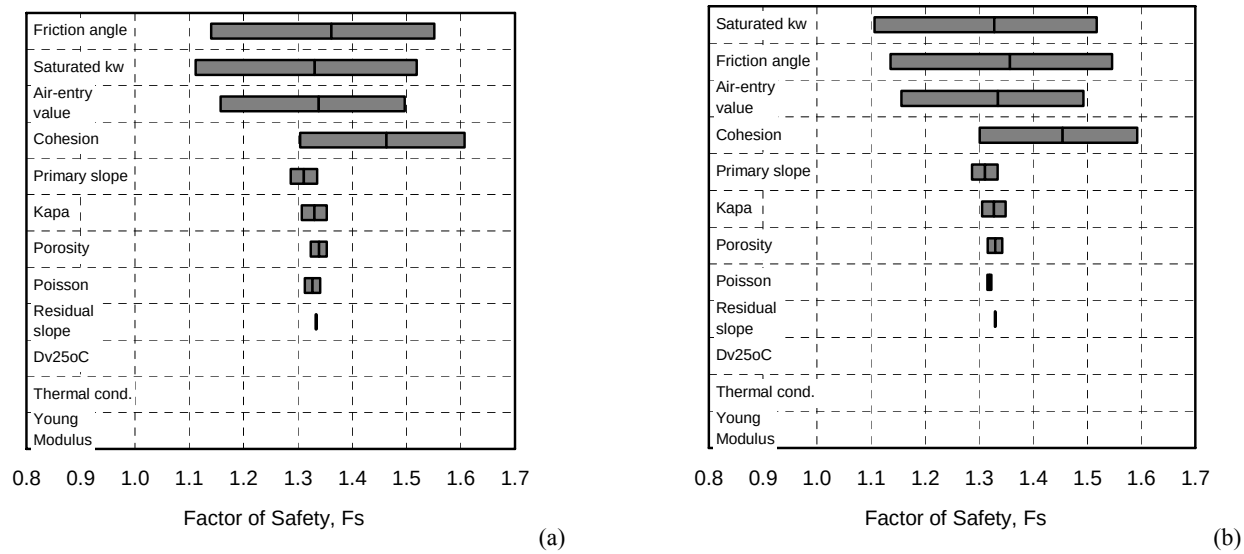

Figure 6. Deterministic tornados at t = 14 days for the low, loam embankment: (a) u_{wmin} = -60 kPa; (b) u_{wmin} = -20 kPa.

Figure 6 shows that the friction angle, the saturated hydraulic conductivity, the air-entry value, and the effective cohesion have important impacts to the uncertainty of the factor of safety. The primary SWCC slope, the unsaturated shear strength parameter, κ, the soil porosity, Poisson's ratio, and the residual SWCC slope have minor effects. The parameters associated with vapour flow, D^{v}_{25oC} and heat flow, λ_s, had no influence whatsoever on the factor of safety. The flow of water during a precipitation event takes place primarily as liquid flow, and the flow of vapour is negligible. Changes in Young modulus had no effect to the factor of safety.

Figure 7 presents probabilistic event tornado diagrams for the low, loam embankments, at t = 14 days. The probabilistic event tornado diagrams are obtained by removing the uncertainty of one variable at a time and computing the resulting variability in the factor of safety. The smaller the size of the bar, the more sensitive is the factor of safety to the input variable corresponding to that bar. Probabilistic event tornado diagrams tend to have a less appealing appearance but are more realistic than deterministic diagrams, since they preserve most of the uncertainty of the model (Clemen, 1996). In summary, a probabilistic event tornado diagram shows how much uncertainty remains in the model if the uncertainty of a single given parameter was eliminated.

Figure 7 confirms that the parameters with the greatest impacts on the factor of safety are the saturated hydraulic conductivity, the effective cohesion, the friction angle, and the air-entry value. The relative sensitivity of the factor of safety to the input parameters does not vary considerably when comparing the initially "dry" and "wet" conditions. The low-impact parameters are the same identified by the deterministic event tornado diagrams.

The difference between the 10th percentile and $F_s = 1$ provides insight into the embankment hazard level. Figure 7 shows that the 10th percentile is close to the unity for the full model and for a large number of variables. This results in a probability of failure near to 10%. The 10th percentile increases considerably when the variability of some "high-impact" variables is removed, such as the variability of the saturated hydraulic conductivity and friction angle.

Figures 8 and 9 present the transient sensitivity of the factor of safety to the input variables based on deterministic event tornado diagrams for the low, loam embankment. The transient sensitivity of F_s to the input parameters is summarized in terms of the size of the bars, computed by subtracting the 90th and 10th factor of safety percentiles. According to Figs. 8 and 9, the friction angle was the variable with the greatest impact throughout the precipitation event. However, the sensitivity of the factor of safety to the friction angle was slightly reduced as the precipitation event advanced. The effective cohesion was the second most important parameter overall, with exception of the last three to four days of the precipitation event. The impact of effective cohesion increased slightly with time.

Several input variables have an impact to the factor of safety that changes considerably with time. The primary SWCC slope and the unsaturated shear strength parameter, κ, appear to have a significant role in the beginning of the precipitation event. However, as time advanced the sensitivity of the factor of safety to the primary SWCC slope and κ reduced, being considered minor past the 4th day and 8th day, respectively.

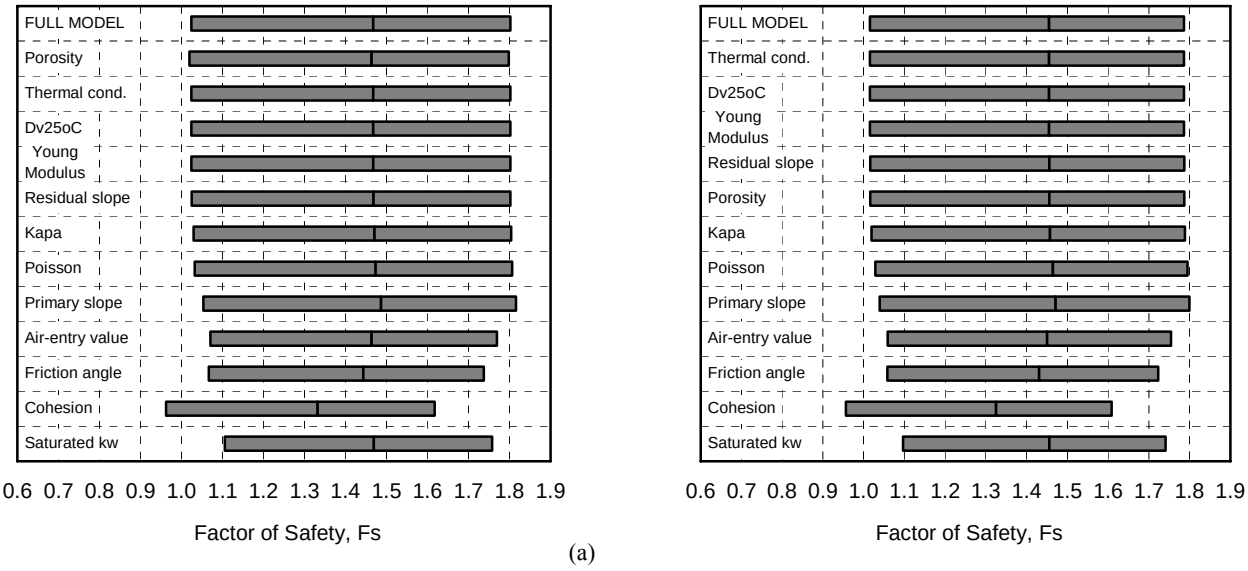

Figure 7. Probabilistic event tornado diagrams at t = 14 days for the low, loam embankment. Initial conditions: (a) $u_{w\ min}$ = -60 kPa; (b) $u_{w\ min}$ = -20 kPa.

The sensitivity of the factor of safety to the air-entry value and to the saturated hydraulic conductivity increased with time. The impact of the hydraulic properties accumulates as the precipitation event advances. It appears that the longer the precipitation event, the higher the sensitivity of the factor of safety to the inherent uncertainty of the saturated hydraulic conductivity. However, the impact of the air-entry value reached a plateau on the 12nd day. The remaining input parameters appear to have relatively small or no influence on the factors of safety for the precipitation event.

Based on the above observations, two distinct stages can be established, regarding the sensitivity of the factor of safety to the input parameters for the low, loam embankment. During the first stage, which extends up to approximately the 7th day, the dominating parameters are (i) the friction angle, (ii) the unsaturated shear strength parameter κ, (iii) the primary SWCC slope, and (iv) the air-entry value. During the second stage, which starts at approximately the 7th day, the input parameters with the greatest impacts are the (i) saturated hydraulic conductivity, (ii) the friction angle, and (iii) the air-entry value.

4.2 Low clay embankment

Figure 10 presents the transient sensitivity of the factor of safety to the input variables based on deterministic event tornado diagrams for the low, clay embankment. According to Fig. 10, the effective cohesion has the greatest impact to the factor of safety up to the fourth day. The saturated hydraulic conductivity became the most important parameter past the fourth day. The soil cohesion, friction angle, soil porosity, Poisson's ratio, and unsaturated shear strength parameter, κ, present roughly constant impacts throughout the precipitation event. However, the sensitivity of the factor of safety to κ slightly decrease as the precipitation event advanced.

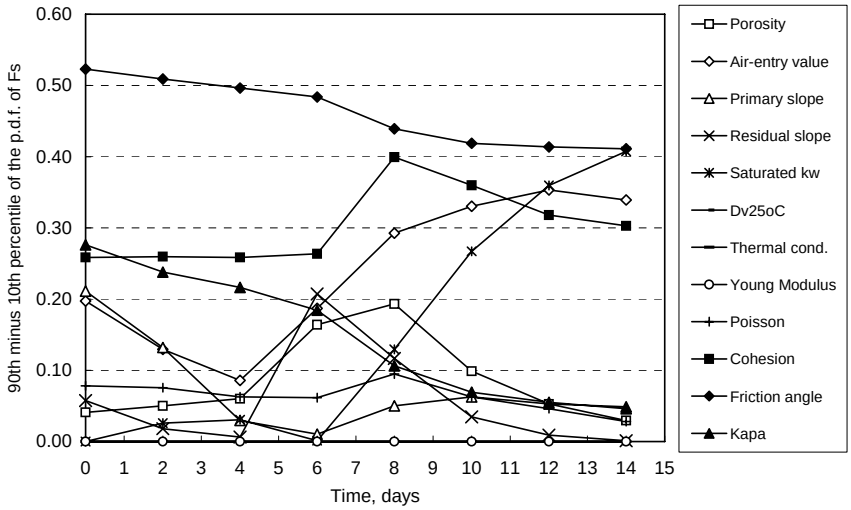

Figure 8. Transient sensitivity based on deterministic event tornado diagrams for the low, loam embankment. Initial conditions: $u_{w\ min}$ = -60 kPa.

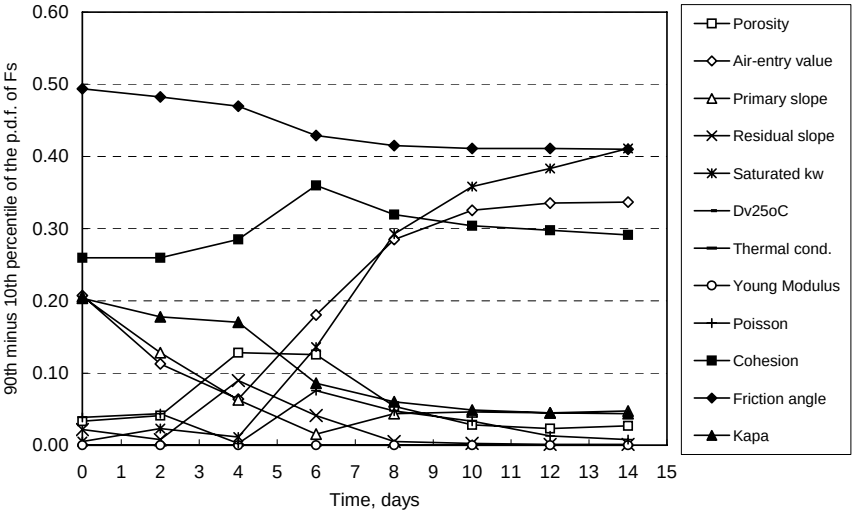

Figure 9. Transient sensitivity based on deterministic event tornado diagrams for the low, loam embankment. Initial conditions: $u_{w\ min}$ = -20 kPa.

The saturated hydraulic conductivity and the air-entry values have time-dependent impacts, similar to the results shown for the loam soils. The sensitivity of the factor of safety to the saturated hydraulic conductivity and the air-entry value increased with time. The influence of both properties accumulates as the precipitation event advanced.

It appears that the longer the precipitation event, the higher the impact of the air-entry value, until a plateau was reached on the sixth day. This plateau appears to indicate that the pore-water pressure distribution has reached near steady state conditions past the fourth and sixth days. The relatively short time required for reaching steady state conditions is due to the low percolation rate that impedes the flow of water across the embankment, towards the water table.

4.3 High loam embankment

Figure 11 presents the results of the sensitivity analysis for the high, loam embankment. According to Fig. 11, the friction angle was the parameter with the highest impact to the factor of safety throughout the precipitation event. The impact of the friction angle was slightly reduced as the precipitation event advanced, but remained the highest. The unsaturated shear strength parameter, κ, was the second most important parameter overall. The high impact of the friction angle is associated with the relatively larger size of the embankment and the relatively high confining stresses. The significance of κ can be explained by the relatively high friction angle. The effective cohesion had an intermediate impact on the factor of safety. This result indicates that the shear strength of the high loam embankment originates primarily from frictional forces.

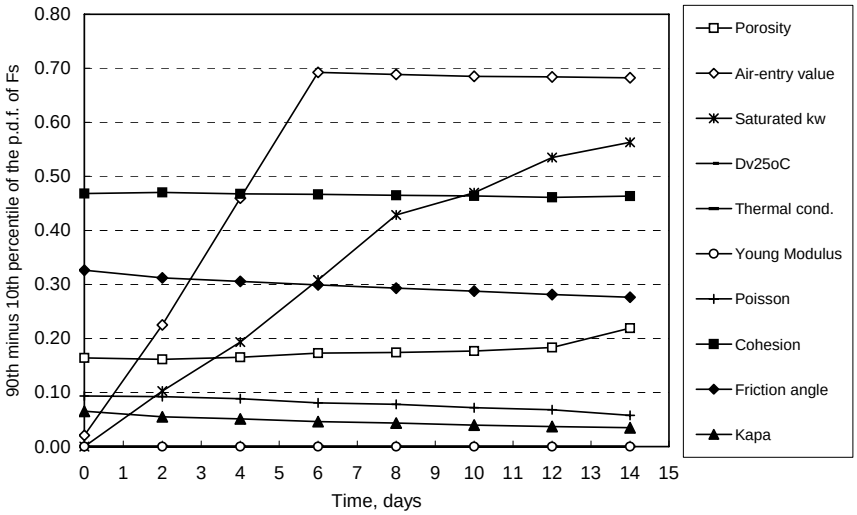

Figure 10. Transient sensitivity based on deterministic event tornado diagrams for the low, clay embankment. Initial conditions: $u_{w\,min}$ = -60 kPa.

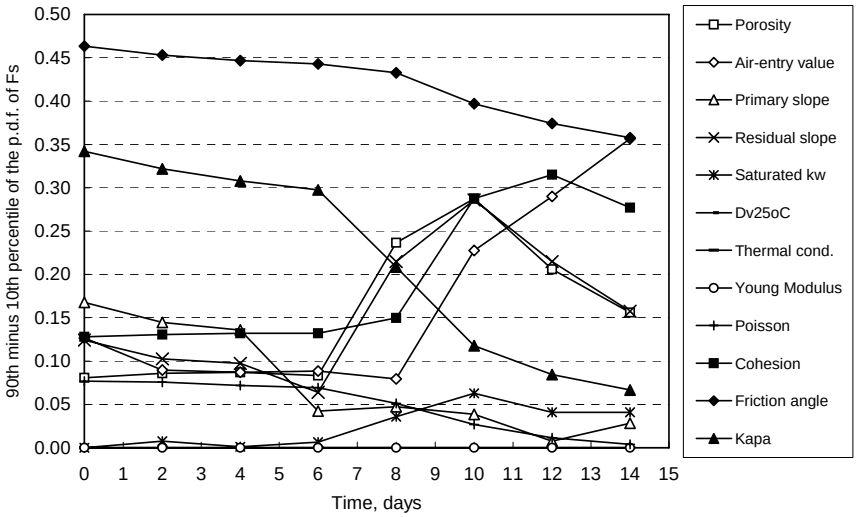

Figure 11. Transient sensitivity based on deterministic event tornado diagrams for the high, loam embankment. Initial conditions: $u_{w\,min}$ = -100 kPa.

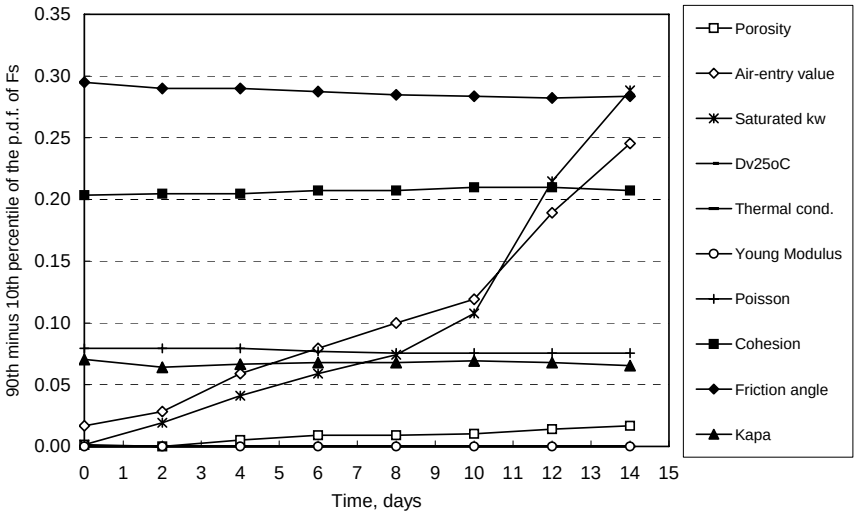

Figure 12. Transient sensitivity based on deterministic event tornado diagrams for the high, clay embankment. Initial conditions: $u_{w\,min}$ = -100 kPa.

Again, several input variables have time-dependent impacts, as observed for the previous embankment configurations. The sensitivity of the factor of safety to the air-entry value and to the saturated hydraulic conductivity increased with time. The impact of the air-entry value is intermediate to low during the beginning of the precipitation event and becomes high by the end of the 14th day. The saturated hydraulic conductivity has a small, but increasing impact.

The time-dependent sensitivity of the factor of safety is a product of the accumulation of the influence of the hydraulic properties as the precipitation event advanced. The longer the precipitation event, the higher the impact of the air-entry value. The impact of the saturated hydraulic conductivity also increases. Soil porosity presented an intermediate to low impact. The remaining input parameters appear to have relatively small or no influence on the factors of safety throughout the precipitation event.

4.4 High clay embankment

Figure 12 presents the transient sensitivity of the factor of safety to the input variables for the high, clay embankment. According to Fig. 12, the friction angle was the variable with the highest impact throughout the precipitation event. However, the impact of the friction angle decreased, due to the considerable decrease in the saturated soil effective stresses. Poisson ratio, unsaturated shear strength parameter, κ, and porosity presented intermediate to low impacts.

All properties have constant impacts throughout the precipitation event, with exception of the air-entry value and the saturated hydraulic conductivity. The sensitivity of the factor of safety to the air-entry value and the saturated hydraulic conductivity increased with time, as observed in the previous embankment configurations. The air-entry value and the saturated hydraulic conductivity have a small but increasing impact during the first 6 days. The sensitivity of factor of safety to both variables increased sharply past the 10th day.

The longer the precipitation event the higher the importance of the air-entry value and the higher the importance of the saturated hydraulic conductivity. The sensitivity of the factor of safety to the air-entry value was particularly high on the 14th day. An increase in the air-entry value may result in near completely saturated initial conditions, explaining the high impact. The remaining input parameters shown in Fig. 12 appear to have relatively small or no influence on the factors of safety throughout the precipitation event.

5 CONCLUSIONS

The fundamental premise of the research presented in this paper is that the understanding of the sensitivity of the factor of safety to saturated and unsaturated soil parameters offers valuable information to geotechnical engineering practice. Geotechnical uncertainty is often approached as a result of imperfections in the models. This is particularly true for problematic, unsaturated soil behavior. However, inherent property uncertainty may often outweigh the uncertainty associated with unsaturated soil models.

The results presented in this article are part of a large research project that focused on the formulation of a decision support system for railway embankment hazard management. The research results on unsaturated slope modeling and unsaturated property variability allowed also the analysis of the sensitivity of the factor of safety to the inherent uncertainty of the soil properties.

It was shown that the uncertainty of the air-entry value has a time-dependent impact on the uncertainty of the factor of safety. The changes in the air-entry value result in changes in several

predicted properties; namely, the hydraulic conductivity function, the vapour conductivity function, the thermal properties, and the unsaturated shear strength envelope. However, the time dependent characteristics of the air-entry value sensitivity suggests that the change in the predicted hydraulic conductivity function is responsible for the high sensitivity of air-entry value.

It appears that most case scenarios could be appropriately modeled without considering the variability of the air-entry value, given that the precipitation event is shorter than 6 days, with exception of the low clay embankment. However, the air-entry value uncertainty is of paramount importance for analyses of longer periods and must be considered as an uncertain, random variable.

The variability of the primary and residual SWCC slopes presented intermediate to low impacts on the factor of safety and may be modeled as certain, fixed values. The uncertainty on the saturated hydraulic conductivity also presents a time-dependent impact on the uncertainty of the factor of safety. The uncertainty of the saturated hydraulic conductivity may be neglected if the duration of the precipitation event is short enough. It appears that most case scenarios could be appropriately modeled without considering the variability of the saturated hydraulic conductivity, given that the precipitation is shorter than 4 days.

The inherent uncertainties of the vapour diffusivity, thermal conductivity, and Young modulus have negligible impacts on the uncertainty in the factor of safety throughout the precipitation event. However, Gitirana Jr. (2005) shows important impact during evaporation periods.

Effective cohesion and friction angle have proven to have high impacts on the factor of safety. The impacts of effective cohesion and friction angle are significantly higher than the impacts of the remaining properties.

Finally, the uncertainty in the unsaturated shear strength parameter, κ, has a high impact on the uncertainty in the factor of safety during early stages of the precipitation event for the loam embankments. However, the impact of κ decreases as the precipitation event advances and the soil suctions decrease. The importance of the uncertainty in κ is relatively low for the clay embankments, due to the low friction angle. Ideally, lower friction angles result in relatively low unsaturated shear strength.

The conclusion regarding κ are dependent on the assumptions regarding the shape of the unsaturated shear strength envelope. A review of the pertinent literature indicates that further research is required for a better characterization and modeling of the unsaturated shear strength of cohesive soils. Nevertheless, the uncertainty modeling approach proposed herein for the unsaturated shear strength envelope provides an efficient framework for addressing the uncertainties associated with the shear strength of unsaturated soils.

6 ACKNOWLEDGEMENTS

The authors would like to thank the "Conselho Nacional de Desenvolvimento Científico e Tecnológico – CNPq", Brazil, NSERC, Canadian Pacific Railway, and Saskatchewan Highways, for financial support during the course of this research.

7 REFERENCES

Baker, R. (1980) Determination of the critical slip surface in slope stability computations. International J. for Num. and Analytical Methods in Geomechanics, 4, 333-359.

Clemen, R.T. (1996) Making Hard Decisions. Duxbury Press, U.S.. 664p.

Fredlund, D.G. e Gitirana Jr., G.F.N. (2005) Keynote Address: Unsaturated Soil Mechanics as a Series of Partial Differential Equations. GEOPROB 2005. Famagusta, Cypurs. 3-30.

Fredlund, D.G. and Rahardjo, H. (1993) Soil Mechanics for Unsaturated Soil. John Wiley & Sons, NY, United States of America, 517p.

Gitirana Jr., G.F.N. (2005) Weather-Related Geo-Hazard Assessment Model for Railway Embankment Stability. PhD Thesis, Department of Civil Engineering, University of Saskatchewan, Saskatoon, Canada, 411p.

Gitirana Jr., G.F.N. and Fredlund, D.G. (2003) Transient embankment stability analysis using dynamic programming. Proceedings of the 56th Canadian Geotechnical Conference, Winnipeg, MB, Canada. 1: 808-814.

Gitirana Jr., G.F.N. and Fredlund, D.G. (2004) Soil-water characteristic curve equation with independent properties. J. of Geot. and Geoenvironl. Engr., ASCE, 130(2): 209-212.

Li, K.S. (1992) Point estimate method for calculating statistical moments. J. of Engr. Mechanics, 118(7): 1506-1511.

PDE Solutions Inc. (2005) FlexPDE 5 - Reference Manual. Antioch, CA, USA.

Rosenblueth, E. (1975) Point estimates for probability moments. Proc. National Academy of Sciences, 72(10): 3812-3814.

SoilVision Systems Ltd. (2003) SoilVision User's Guide. Version 4.0. Saskatoon, SK, Canada.

Transportation Safety Board. (1997) Interim railway safety recommendations concerning the identification and detection of railway roadbed instability. TSB Recommendation # 05/97. Transportation Safety Board, Quebec, Canada.